PHYSICAL REVIEW B VOLUME 14, NUMBER 11 1 DECEMBER 1976

Solidification of ^{4}He monolayer*

Michael A. Lee, D. N. Lowy, and Chia-Wei Woo
Department of Physics, Northwestern University, Evanston, Illinois 60201
(Received 19 April 1976)

We apply a variational method to calculate ground-state properties of a ^{4}He monolayer on a neutral substrate. A stable solid phase occurs at densities above 0.091 Å^{-2}. The melting density is about 0.095 Å^{-2} and the freezing density is about 0.085 Å^{-2}, which is about 5% higher than the observed freezing density. We also describe an improved method for solving the Percus-Yevick equation.

I. INTRODUCTION

For some time now one of the exciting areas of research in low-temperature physics has been helium monolayers physically adsorbed on crystalline substrates. There are good reasons for it. First, these monolayers make good models for two-dimensional systems. Next, one of the thermodynamic variables: the areal density, $n \equiv N/A$, can be varied at will from zero to values equivalent to those of bulk solid helium. Furthermore, the system undergoes a large variety of phase transitions, some characteristic of two-dimensional systems, and others under the influence of the substrate field. One of the earlier experimental difficulties, that of preparing clean, homogeneous, inert substrate surfaces, was overcome with the advent of "Grafoil." A lucid account of thermodynamic measurements conducted on helium adsorbed on grafoil can be found in a long article by the University of Washington group.[1]

To a theoretician, adsorption begins with an ideal substrate and a single atom (molecule). The substrate provides a potential well in the direction normal to its surface. Adsorption takes place if the atom has at least one bound state in the well. This appears to be a deceptively simple problem. Actually even a perfect crystal with a sharply cleaved surface presents to the adatom a complicated potential. In principle, one wishes to solve for bound states in the normal direction and band structure in the lateral directions. However, since the adsorption potential is far from separable into normal and lateral parts, the motions in and out of the plane of the adsorption surface are strongly coupled. Furthermore, the substrate is not static. It has excitations. The atom scatters virtually against the substrate surface and finds itself dressed by these excitations. Thus it acquires an effective mass. When one progresses to two or more atoms, further complications arise. In particular, the interaction between the atoms becomes renormalized by the substrate excitations, and one obtains effective interactions which are more often than not nonlocal.

Fortunately in the case of helium adsorbed on grafoil most of these complications are harmless. The periodic lateral variations of the adsorbing potential are weak, in the sense that single-particle band structures exhibit wide bands and narrow gaps[2] so that the helium atoms possess almost total surface mobility even at low temperatures. The adsorbed layer is practically two dimensional in that the range of motion in the normal direction is small compared to all relevant characteristic lengths. Experimentally measured heat capacities for low-density ^{4}He and ^{3}He layers thus adsorbed display well-known ideal Bose and Fermi gas characteristics.[1] The situation becomes even more encouraging when one discovers that the grafoil substrate turns out to be very inert. The single-particle effective mass is not far from the bare mass. Taking the interaction to be bare Lennard-Jones, Siddon and Schick[3] were able to fit low-density experimental data remarkably well to results deduced from a low-order virial expansion.

Also, an attempt was made by Novaco and Campbell[4] to include the effects of the periodic variation and normal extent of the substrate potential for helium on graphite. The authors concluded that the effective two-dimensional potential "differs slightly" from the bare potential and the calculated equilibrium energy and density are within a few percent of those calculated with two-dimensional models. Furthermore, "the effect of the periodic potential is very small," being of the order of 3% at equilibrium.

These observations lead to the conclusion that helium monolayers physisorbed on grafoil can be represented faithfully by a simple model of bare helium atoms confined to two dimensions. At intermediate densities, the system must be treated as a (two-dimensional) quantum liquid which at a still higher density undergoes a liquid-solid transition.

Several calculations, all variational in nature,

have appeared in the literature[5-8] concerning the binding energy of ^{4}He monolayers at densities below 0.060 Å^{-2}. The results obtained using vastly different techniques including integral equations, molecular dynamics, and Monte Carlo all fell within a few percent. The equilibrium density at 0.035–0.040 Å^{-2} is very low when scaled and compared against the bulk density of 0.022 Å^{-3}. The binding energy at the equilibrium density is only about 0.6 K per particle. At densities between 0.036 and 0.056 Å^{-2}, the excitation spectra have been calculated,[9] leading to heat capacities at finite temperatures which are in good agreement with experiment.[10] Our understanding is therefore quite good in this range of densities.

Very little has been done at higher densities leading to the two-dimensional solid phase. It is known from experiment[1] that the ^{4}He monolayer completes at about 0.115 Å^{-2}, and that the liquid-solid transition takes place at about 0.080 Å^{-2}. A recent paper by Liu, Kalos, and Chester[11] reports that variational calculations using Monte Carlo integration techniques result in a melting density of 0.077 Å^{-2} and a solidification density of 0.061 Å^{-2}. We wish to present in this paper results of variational calculations obtained with a totally different technique. The procedure used here for the two-dimensional solid is adapted from a new and rather novel method developed by us[12] for bulk quantum crystals. Our long-term plan is to follow with calculations of excitation spectra in the solid phase, and then combining these results with earlier work[3,6,9] come up with a detailed theoretical account of the monolayer phase diagram.

A comment on the distinction between two kinds of "solid" phases is in order before we proceed. Let us for the moment assume that the substrate displays a noticeable surface lattice structure. A completely filled lattice will then look like a solid layer in registry with the substrate periodicity.[4] It is not a *real* solid, although there is no qualitative way to differentiate an Einstein solid from such a filled lattice gas: Each adatom moves independently in a harmonic well, even though the harmonic well arises from different sources in the two cases. The solid phase with which we are concerned is the one whose existence relies on correlation effects between the adatoms. The substrate periodicity modifies, but does not control, the crystallization process. The method proposed here will require only minor adaptations to account for such modifications.

II. THEORY

Even though the formulation of our theoretical method has been published elsewhere, we present here a brief summary for completeness.

For a system of N ^{4}He atoms confined to an area A and described by the Hamiltonian

$$H=\sum_{i=1}^{N}-\frac{\hbar^2}{2m}\nabla_i^2+\sum_{i<j=1}^{N}V(r_{ij}), \tag{1}$$

where $V(r)$ is the Lennard-Jones potential

$$V(r)=4\epsilon\left[(\sigma/r)^{12}-(\sigma/r)^6\right],$$
$$\epsilon=10.22\ \text{K},\quad \sigma=2.556\ \text{Å}, \tag{2}$$

a useful form for the variational wave function is the Hartree-Jastrow product:

$$\psi(\vec{r}_1,\vec{r}_2,\ldots,\vec{r}_N)=\prod_{i=1}^{N}\varphi(\vec{r}_i)\prod_{j<k=1}^{N}f(r_{jk})$$
$$\equiv\prod_{i=1}^{N}\varphi(\vec{r}_i)\prod_{j<k=1}^{N}e^{u(r_{jk})/2}. \tag{3}$$

In an earlier work[13] the single-particle factor $\varphi(\vec{r}_i)$ is taken to be constant for the liquid phase, and a Gaussian centered about lattice site $\vec{R}_i$ in the solid phase. This is also what is done in Ref. II for ^{4}He monolayers. The solid wave function is not properly symmetrized, but this is not crucial for systems in which the binding energy does not depend sensitively on quantum statistics. Nevertheless, in our new method we find it unnecessary to leave ψ unsymmetrized. By writing $\varphi(\vec{r})$ in the form:

$$\varphi(\vec{r})=\exp\left(\frac{1}{2}\sum_{\vec{G}}t_{\vec{G}}\,e^{i\vec{G}\cdot\vec{r}}\right), \tag{4}$$

where $\{\vec{G}\}$ represents a set of reciprocal vectors of the specified lattice, we have properly accounted for the Bose statistics. The coefficients $\{t_{\vec{G}}\}$ will serve as variational parameters. $\{t_{\vec{G}}\}=0$ corresponds to a liquid phase, while for a solid phase at least the leading $t_{\vec{G}}$ must be nonzero. This leading $t_{\vec{G}}$ maximized $\varphi(\vec{r})$ at *every* lattice site, while the higher-order $t_{\vec{G}}$'s affect the shape of $\varphi(\vec{r})$ about each lattice site. Such a single-particle factor is completely general.

In terms of the trial wave function given in Eq. (3), the expectation value of H can be expressed in the exact form

$$E=\frac{1}{2}\int P^{(1)}(\vec{r}_1)\left(-\frac{\hbar^2}{4m}\nabla_1^2 t(\vec{r}_1)\right)d\vec{r}_1$$
$$+\frac{1}{2}\int P^{(2)}(\vec{r}_1,\vec{r}_2)$$
$$\times\left(V(r_{12})-\frac{\hbar^2}{4m}\nabla_1^2 u(r_{12})\right)d\vec{r}_1\,d\vec{r}_2, \tag{5}$$

where $P^{(1)}(\vec{r}_1)$ and $P^{(2)}(\vec{r}_1,\vec{r}_2)$ are the one- and two-particle distribution functions defined by

$$P^{(1)}(\vec{r}_1) = \frac{N}{Z}\int d\vec{r}_2 d\vec{r}_3 \cdots d\vec{r}_N |\psi|^2, \tag{6}$$

$$P^{(2)}(\vec{r}_1, \vec{r}_2) = \frac{N(N-1)}{Z}\int d\vec{r}_3 \cdots d\vec{r}_N |\psi|^2, \tag{7}$$

and

$$Z = \int |\psi|^2 d\vec{r}_1 \cdots d\vec{r}_N .$$

Instead of using a cluster expansion to evaluate Eqs. (6) and (7) in terms of integrals involving $\varphi(\vec{r})$ and $f(r)$, as has been customary, we employ integral equations of the Bogoliubov-Born-Green-Kirkwood-Yvon (BBGKY)[14] and Percus-Yevick (PY)[15] type.

$$\vec{\nabla}_1 P^{(1)}(\vec{r}_1) = P^{(1)}(\vec{r}_1)\vec{\nabla}_1 t(\vec{r}_1) + \int P^{(2)}(\vec{r}_1, \vec{r}_2)\vec{\nabla}_1 u(r_{12})\, d\vec{r}_2 \tag{8}$$

and

$$g(\vec{r}_1, \vec{r}_2) = e^{u(r_{12})} + e^{u(r_{12})}\int d\vec{r}_3 [1 - e^{-u(r_{13})}] g(\vec{r}_1, \vec{r}_3) \times [g(\vec{r}_2, \vec{r}_3) - 1] P^{(1)}(\vec{r}_3), \tag{9}$$

where we define

$$\varphi^2(\vec{r}) = e^{t(\vec{r})} . \tag{10}$$

Using the relation

$$g(\vec{r}_1, \vec{r}_2) = P^{(2)}(\vec{r}_1, \vec{r}_2)/[P^{(1)}(\vec{r}_1) P^{(1)}(\vec{r}_2)], \tag{11}$$

Eqs. (8) and (9) become a closed set. $P^{(1)}$ and $P^{(2)}$ can then be solved for each choice of the trial wave function. In an actual application one might begin with Eq. (9) and take $P^{(1)}(\vec{r}_1) = n$, the mean number density. The equation then reduces to the familiar PY equation[15] for a quantum liquid, and $g(\vec{r}_1, \vec{r}_2)$ reduces to $g(r_{12})$, a radial distribution function. Equation (8) may then be solved with $P^{(2)}(\vec{r}_1, \vec{r}_2) = P^{(1)}(\vec{r}_1) P^{(1)}(\vec{r}_2) g(r_{12})$ and the resulting $P^{(1)}(\vec{r}_1)$ entered into Eq. (9) to obtain an improved $g(\vec{r}_1, \vec{r}_2)$. The process should be continued until convergence. For practical pruposes one stops at one iteration. The results will already be better than the usual truncated cluster-expansion procedures which take $P^{(1)}(\vec{r}) = \varphi^2(\vec{r})$ and $g(\vec{r}_1, \vec{r}_2) = f^2(r_{12})$.

Having calculated $P^{(1)}(\vec{r})$ and $P^{(2)}(\vec{r}_1, \vec{r}_2)$, we may immediately obtain the energies for both the liquid and solid phases using Eq. (5).

To solve the first BBGKY [Eq. (8)], we first expand $P^{(1)}(\vec{r})$ in the series:

$$\ln\left(\frac{P^{(1)}(\vec{r})}{n}\right) = \sum_{\vec{G}} b_{\vec{G}} e^{i\vec{G}\cdot\vec{r}} \tag{12}$$

and also in the more transparent but less rapidly convergent form:

$$P^{(1)}(\vec{r}) = n\sum_{\vec{G}} a_{\vec{G}} e^{i\vec{G}\cdot\vec{r}} . \tag{13}$$

During the first iteration, Eq. (8) reduces to

$$b_{\vec{G}} = t_{\vec{G}} + a_{\vec{G}} F(G), \tag{14}$$

where

$$F(G) = \frac{-2\pi}{G} n \int r g(r) J_1(Gr) u'(r)\, dr \tag{15}$$

and $J_1(Gr)$ is a Bessel function. Equations (12)–(15) form a set of transcendental equations which can be solved for the expansion coefficients $a_{\vec{G}}$ and $b_{\vec{G}}$ given any choice of the variational parameters $\{t_{\vec{G}}\}$ and $u(r)$.

The central point of this procedure is to evaluate the energy at selected density in such a way as to minimize it as a function of the variational functions $u(r)$ and $t(r)$. The energy expression

$$\frac{E}{N} = \frac{1}{N}\int g(r_{12}) P^{(1)}(\vec{r}_1) P^{(1)}(\vec{r}_2) \times \left(V(r_{12}) - \frac{\hbar^2}{4m}\nabla^2 u(r_{12})\right) d\vec{r}_1 d\vec{r}_2 + \frac{1}{N}\int P^{(1)}(\vec{r}_1)\nabla_1^2 t(\vec{r}_1)\, d\vec{r}_1 \tag{16}$$

can be further reduced by defining another correlation function

$$g_E(r_{12}) = \frac{1}{n^2}\frac{1}{2\pi V}\int d\Omega_{12}\int d\vec{r}_2 P^{(1)}(\vec{r}_2) P^{(1)}(\vec{r}_{12} + \vec{r}_2), \tag{17}$$

which is just the average two-particle correlation function for a crystal of bosons which are correlated with a lattice but not with one another. In terms of the Fourier coefficients $g_E(r)$ is written

$$g_E(r) = \sum_{\vec{G}} a_{\vec{G}} a_{-\vec{G}} J_0(Gr) . \tag{18}$$

Our final expression for the energy is then

$$\frac{E}{N} = \frac{n}{2}\int g_E(r_{12}) g(r_{12}) \left(V(r_{12}) - \frac{\hbar^2}{4m}\nabla^2 u(r_{12})\right) d\vec{r}_{12} + \sum_{\vec{G}} \frac{\hbar^2}{8m} a_{\vec{G}} t_{\vec{G}} G^2 . \tag{19}$$

The foremost advantage of this procedure is the absence of the many approximations common in other approaches. The wave function to be optimized is of course approximate. We include one- and two-particle correlation factors but neglect three- and higher-order correlation factors. Since we are really interested in calculating the energy difference between the liquid and solid

phases, the effect of higher-order terms, which are small to begin with, are expected to cancel to a large extent.

Secondly, we approximate the two-particle distribution function $P^{(2)}(\vec{r}_1, \vec{r}_2)$ by $P^{(1)}(\vec{r}_1)P^{(1)}(\vec{r}_2)g(r_{12})$, where g is the radial distribution function for the liquid phase. This is the only other approximation in the theory. It includes the essential short-range correlations, leaving the long-range correlations entirely in $P^{(1)}(\vec{r})$. What this approximation neglects is that g should contain correction terms which possess the symmetry of the crystal. The fact remains, however, that it is $P^{(2)}$, rather than g, which determines $P^{(1)}$, and it is $P^{(2)}$ that one uses in calculating the energy. The major difference between the liquid and solid phase is that $P^{(1)}(\vec{r})$ peaks about the lattice sites. On physical grounds it is entirely reasonable to hope that the desired correlations are already accounted for in $P^{(1)}(\vec{r})$.

III. RESULTS AND DISCUSSION

Appendix A shows how the PY equation is reduced to a practical form, and Appendix B discusses the existence of and convergence of solutions.

We searched for minima in the energy expression Eq. (16) by varying our parameters $t_{\vec{G}}$ and $u(r)$. If for a given density the absolute minimum in the energy is obtained only when all the $t_{\vec{G}}$'s are identically zero, we may conclude that no periodic configuration is stable with respect to the liquid configuration. We denote the minimum liquid energy by E_L. Conversely if there exist some nonzero values for the set of $t_{\vec{G}}$ such that the energy of this periodic configuration is less than E_L, this particular solid structure will be stable with respect to the liquid. The minimum solid energy is denoted by E_S.

We gave $u(r)$ the functional form $-(d\sigma/r)^5$ where d is a variational parameter. The lattice structure we used was close packed. From our experience with bulk ^{4}He, we retained only the first nontrivial $t_{\vec{G}}$ (corresponding to $|\vec{G}|$ equal to the nearest-neighbor distance in reciprocal space), which we relabel τ. We retained values of the coefficients $a_{\vec{G}}$, $b_{\vec{G}}$, and $F(G)$ for $|\vec{G}|$ out to the tenth-nearest-neighbor distance. This retained 50 terms in the Fourier expansion for the close-packed lattice structure.

Denote the value of the energy in the two-dimensional parameter space $[d, \tau]$ by $E(\tau, d)$. For densities below 0.091 Å^{-2} we found that the absolute minimum of $E(\tau, d)$ occurred at $\tau = 0$, corresponding to a stable liquid phase. However at $n = 0.091$ Å^{-2} we found that

$$E(\tau = 0.18,\ d = 1.15494) = E(\tau = 0,\ d = 1.19012)$$

that is $E_S = E_L$, and for n greater than 0.091 Å^{-2} we actually found that E_S was a few tenths of a degree less than E_L (out of a total energy of 3 K or more). The width of the two-phase coexistence region is uncertain, but estimated to be about $\Delta n \approx 0.005$ Å^{-2}. Thus the melting density is about 0.095 Å^{-2} and the freezing density is about 0.085 Å^{-2}. The energy of the solid is estimated to be about +3.25 K.

The results of our calculation are best shown graphically. Figure 1 shows the liquid energy E_L plotted against the density n in comparison to the results obtained by Miller, Woo, and Campbell.[6] Note that while at low density the agreement is quite good, there is a discrepancy of as much as 0.2 K at $n = 0.056$ Å^{-2}: the highest density reached in Ref. 6. The source of the discrepancy lies in the use of a BBGKY equation in Ref. 6, and the use of the PY equation in this work. Note that in determining the solidification density we need only the energy difference between E_S and E_L and for this quantity such errors should largely cancel.

Figure 2 shows that the two-particle distribution function obtained by the two different methods is in excellent agreement at the equilibrium density. This is encouraging since $g(r)$ plays a major role in the determination of $P^{(1)}(\vec{r})$.

Figures 3–5 exhibit energies as functions of τ for families of the Jastrow function. Figure 3, at density $n = 0.073$ Å^{-2} (deep in the liquid-phase region), shows no energy minimum except at $\tau = 0$. There is no tendency of solidification. Figure 4, at density $n = 0.091$ Å^{-2} (just about the transition point), shows a clear minimum at finite τ which is approximately equal to E_L (or minimum E at $\tau = 0$). Figure 5, at density $n = 0.10$ Å^{-2} (above the solidification density), shows exaggerated behavior at

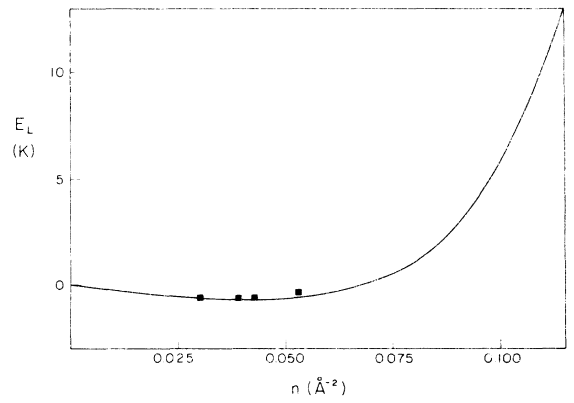

FIG. 1. Liquid energy E_L as a function of density n. Solid curve shows our values; points show the values obtained by Miller *et al.* (Ref. 5).

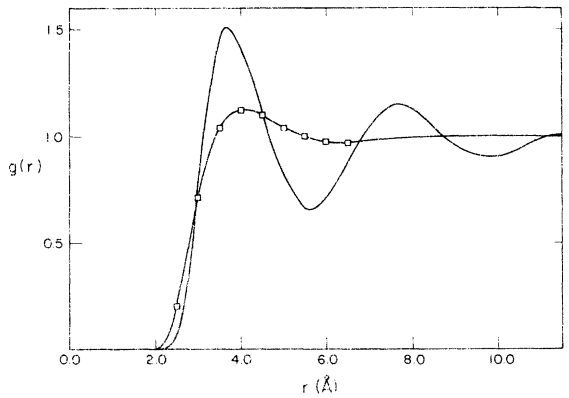

FIG. 2. Pair distribution function $g(r)$ at the densities 0.037 and 0.09 Å^{-2} plotted against radial distance r. Solid line shows our values; the points the values obtained by Miller *et al.* (Ref. 5).

finite τ. The fact that E_S actually drops below E_L is a result of the solid wave function (τ finite) partially including three- and more particle correlation effects, while the liquid wave function ($\tau = 0$) contains only Jastrow or two-particle correlation effects.

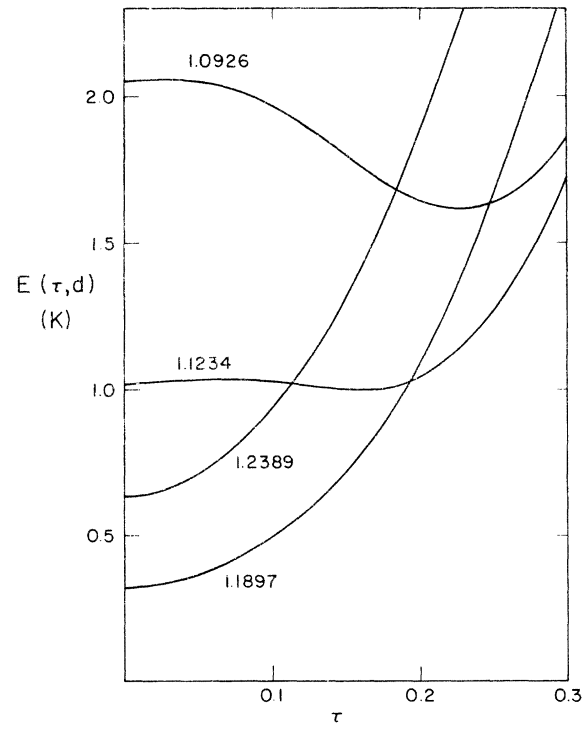

FIG. 3. Energy at the density 0.073 Å^{-2} as a function of the single-particle parameter τ, for values of the Jastrow parameter d as labeled. Note absolute minimum at $\tau = 0$. This implies a stable liquid phase.

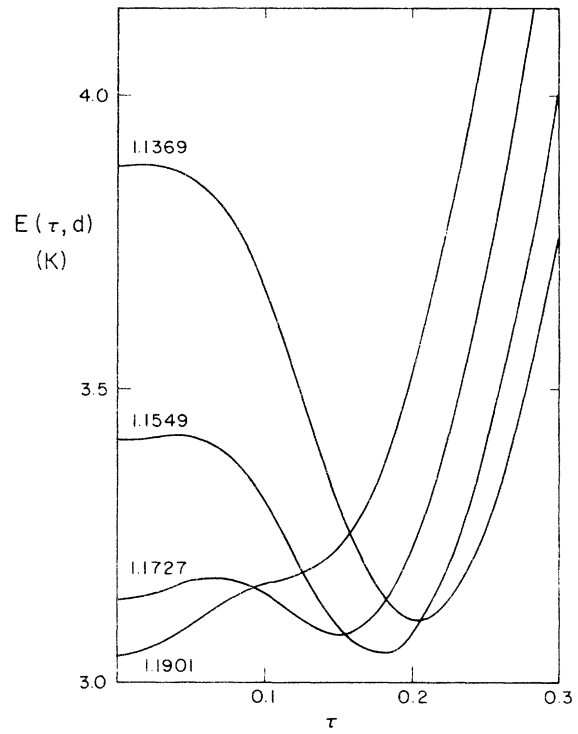

FIG. 4. Energy at the density 0.09 Å^{-2} as a function of τ for four values of d. Note minima at $\tau = 0$ and $\tau \approx 0.18$, so that the solid and liquid energies are equal. This shows the emergence of the solid phase.

Our calculated value for the freezing density is about 5% higher than that observed experimentally, which is in turn about 5% higher than the density predicted by Liu *et al.*[11] using Monte Carlo methods to compute the variational energies. Our agreement with experiment is better than for our bulk ^{4}He calculation which predicted densities about 10% too high. Our model contains no substrate and this may be a source of some of the discrepancy. Any remaining discrepancy would have to arise from the approximations used in obtaining the two-particle correlation function, g.

We are encouraged by the results reported in this paper, and are moving in several new directions. First, we intend to calculate the excitation spectrum in the monolayer solid phase. This is particularly useful for Namaizawa's[16] model calculation of the Kapitza resistence. Next, we wish to include an external one-particle potential which contains lateral periodic variations, so as to study the transitions between lattice-gas solids, liquid, and Debye solid phases. Finally, we shall apply the method to studying the phase transitions in physisorbed H_2 monolayers, which are interesting as precursor states to atomic and molecular hydrogenation of metallic surfaces.

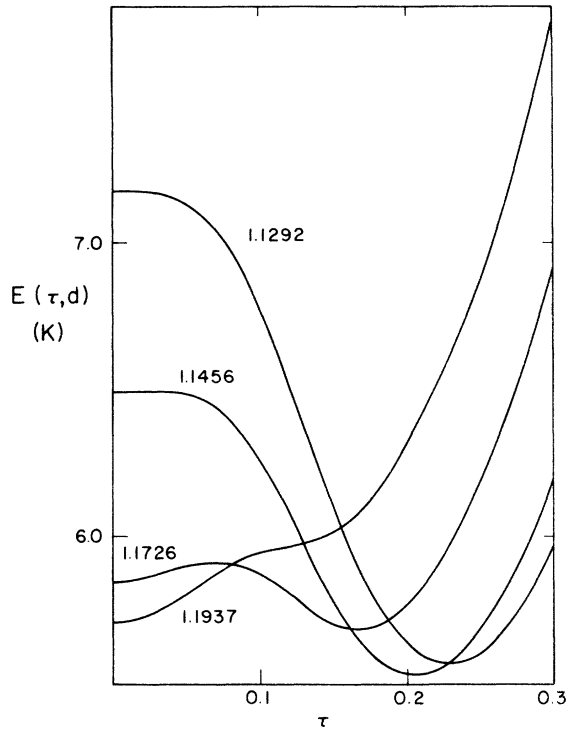

FIG. 5. Energy at the density 0.010 Å^{-2} as a function of τ for four values of d. Note the absolute minimum at $\tau = 0.2$. This lies below the minimum liquid energy and implies a stable solid phase.

ACKNOWLEDGMENT

We wish to acknowledge many illuminating discussions with Y. R. Lin-Liu.

APPENDIX A: PERCUS-YEVICK EQUATION IN TWO DIMENSIONS

The PY equation for an inhomogeneous system is

$$g(\vec{r}_1,\vec{r}_2) = e^{u(r_{12})} + e^{u(r_{12})} \int d\vec{r}_3 P(\vec{r}_3)(1-e^{-u(r_{13})}) \times g(\vec{r}_1,\vec{r}_3)[g(\vec{r}_2,\vec{r}_3)-1]. \quad \text{(A1)}$$

This equation is nearly tractable on modern computing machines if one expands $g(r)$ and $P^{(1)}(\vec{r})$ in Fourier series. We only solve it for the case $P^{(1)}(\vec{r}) = n$. In this case $g(r)$ is translationally invariant and the numerical problem is quite manageable.

Defining $G(r_{12}) = g(r_{12})\, e^{-u(r_{12})}$, the PY equation reduces to the form (after a change of variables)

$$G(r) = 1 + n \int d\vec{s}(e^{u(s)}-1)G(s) \times [G(|\vec{r}-\vec{s}|)\, e^{u(|\vec{r}-\vec{s}|)} - 1]. \quad \text{(A2)}$$

In solving equations such as Eq. (A1) it is quite common to take $g(r)$ to be identically zero for r less than some hard-core radius r_c. In this case $g(r)\, e^{-u(r)}$ is of course also identically zero even if $e^{-u(r)}$ diverges in the limit r goes to zero. We have found that in solving the PY equation in the form (A2), the value of $G(r<r_c)$ is greater than one, and affects G globally. We accordingly conclude that the short-range behavior of $g(r)$ is important and cannot be neglected. By working with $G(r)$ rather than $g(r)$ one obtains the added advantage of working with a relatively smooth function which lends itself to more accurate numerical integration.

In the three-dimensional PY equation the $\vec{s}$ integration can be reduced to a single radial integration. In two dimensions, however, these equations cannot be simplified in this way. To know $g(r)$ at M points one must do a calculation whose length is proportional to M^2 in three dimensions (3-D) but to M^3 in two dimensions (2-D). We have developed a method to decrease this by a factor of 2 to 5 depending on the accuracy required.

The angular integration in the 2-D PY equation can be written in the form

$$\int_0^{2\pi} d\theta\, G((r^2+s^2-2rs\cos\theta)^{1/2}) \times \exp[u((r^2+s^2-2rs\cos\theta)^{1/2})]. \quad \text{(A3)}$$

This is the time-consuming integral which occurs in 2-D but not 3-D. A change of variables to $t^2 = r^2+s^2-2rs\cos\theta$ clearly shows that for uniform accuracy the number of points in the integration should depend on r and s. The integral in the t variable is informative although useless. Most of the numerical error associated with taking too few points is attributable to the rapidly varying nature of e^u rather than G, the latter being quite smooth. Therefore, it would probably be sufficient to sample G at only five or ten points in the angular integration but e^u must be sampled much more often.

We expand

$$\int_0^{2\pi} d\theta\, G((r^2+s^2-2rs\cos\theta)^{1/2}) \times \exp[u((r^2+s^2-2rs\cos\theta)^{1/2})] \simeq \sum_{i=1}^{L} G((r^2+s^2-2rs\cos\theta_i)^{1/2})\, W_i(r,s), \quad \text{(A4)}$$

where

$$W_i(r,s) = \int_{(i-1)2\pi/L}^{2\pi i/L} d\theta \exp[u((r^2+s^2-2rs\cos\theta)^{1/2})] \tag{A5}$$

and θ_i denotes the Chebychev integration points. The sum is over equally spaced points with the weights W_i. While in principle we could improve the accuracy for a given number of points by using a Gaussian integration, in practice this is not feasible since the zeros and weights for the polynomials would have to be determined numerically. When used in conjunction with the technique of scaling the W_i become independent of density.

Another time-saving technique employed was that of "scaling." It is well known that the PY equation scales. If the Jastrow factor $u(r)$ is parametrized with M parameters, say, $\{d_i\}$, $i=1,M$, then $g(r)$ depends on $M+1$ parameters, n and $\{d_i\}$. The dependence on one of these parameters may be eliminated if we choose the parametrization such that $u(r)$ is only a function of the ratios d_i/r, $i=1,M$, that is $u(d_1/r, d_2/r, \ldots, d_M/r)$. By changing variables in the PY equation (21) to $R=r/d_1$, $S=s/d_1$ one obtains

$$G(d_1R) = 1 + n d_1^2 \int d\vec{S} \left\{ \exp\left[u\left(\frac{1}{S}, \frac{d_2/d_1}{S}, \ldots, \frac{d_M/d_1}{S}\right)\right] - 1 \right\} \times G(d_1 S) \left\{ G(d_1|\vec{R}-\vec{S}|) \exp\left[u\left(\frac{1}{|\vec{R}-\vec{S}|}, \ldots, \frac{d_M/d_1}{|\vec{R}-\vec{S}|}\right)\right] - 1 \right\}. \tag{A6}$$

By defining $\tilde{n} = n d_1^2$ and choosing as our unknown $\tilde{G}(R) = G(d_1R)$ we see that $\tilde{G}$ depends on $\tilde{n}$ and d_i/d_1, $i=2,M$, that is on one less parameter. It is not necessary to "unscale" G to calculate the energy. The liquid energy may be written

$$\frac{E}{N} = \frac{1}{2}\frac{\tilde{n}}{d_1^2} \int dR\, g(d_1R) \times \left\{ 4\epsilon \left[d_1^{12}\left(\frac{\sigma}{R}\right)^{12} - d_1^6\left(\frac{\sigma}{R}\right)^6 \right] - \frac{\hbar^2}{4m}\nabla_R^2 u\left(\frac{1}{R}, \frac{d_2/d_1}{R}, \ldots, \frac{d_M/d_1}{R}\right) \right\}. \tag{A7}$$

APPENDIX B: EXISTENCE AND CONVERGENCE OF SOLUTIONS

It is known in the classical case that the PY integral equations do not possess a solution for certain classes of $-V(r)/kT$, or in our quantum notation, for certain classes of $u(r)$. Watts[17] has published a very informative study on the solutions of the PY equation for a classical Lennard-Jones fluid. He offers a tantalizing interpretation for the region of (T,ρ) space where the solution does not exist, by identifying it with the liquid-gas coexistence region of the fluid.

In our work, solving for the radial distribution function of the quantum liquid with a Jastrow factor like $u(r) = -(d\sigma/r)^5$ is identical to solving the PY equation for the classical $kT(d\sigma/r)^5$ repulsive potential. We could not easily carry out an analysis analogous to that of Watts since our solution depends only on the one parameter, $\tilde{n}$, as opposed to the Lennard-Jones fluid which has the two parameters T and ρ. We did, however, determine that a solution ceases to exist near $\tilde{n} \cong 0.11$. The significance of this is in the case of quantum liquids remains to be investigated.

Before discovering that there are indeed regions where solutions are nonexistent, we thought we were having convergence difficulties at high densities, a common malady. This resulted in the development of a method for improving the convergence. The method also provides in a limited way, a test for the existence of a solution.

In solving the PY equation [Eq. (A2)], one commonly begins with some guess for G, which we might denote by G_{in}. One then calculates G_{out} which is defined by

$$G_{\text{out}}(r) = 1 + n \int ds (e^{u(s)} - 1) G_{\text{in}}(s) \times [G_{\text{in}}(|\vec{r}-\vec{s}|) e^{u(|\vec{r}-\vec{s}|)} - 1]. \tag{B1}$$

One could then repeat the procedure using G_{out} as the new G_{in} in the next iteration.

The most common method used to improve convergence (or often to obtain it at all) is to generate the next guess for G_{in} by taking a linear combination of the previous input-output pair. Thus if G_0 is some input guess (usually obtained from a previous iteration) and G_1 is its output, then the next G_{in} is taken to be

$$G_{\text{in}}(r) = \alpha G_0(r) + (1-\alpha) G_1(r), \tag{B2}$$

where α is the "mix," $\alpha = 0$ corresponding to straight iteration and $\alpha = 1$ corresponding to a simple regeneration of G_{out} as G_1.

One would of course like to choose that value of α, which ensures the most rapid convergence.

This optimum value will in general be different after each iteration. The value of α has generally been rather arbitrarily restricted to lie between zero and one. Since the closer α is to unity the less new G is mixed in for the next iteration, the common practice has been that the more difficult the convergence the closer α was chosen to one.

We have developed a procedure for choosing the best possible α before each iteration. We find that not only is the best α not necessarily close to unity, it is often not even within the interval zero to one. What one does with Eq. (B2) is to generate a line in a "function space," each $G_{\text{in}}(\alpha)$ being a point on the line passing through G_0 and G_1. The "best" α would be the one which minimized the "distance" from the true solution to the point on the line determined by α. Obviously α can take on any value in the range $(-\infty, +\infty)$. The best α depends on G_0 and G_1, and hence changes after each iteration. By keeping α close to but less than one, one is not even assured of iterating toward a solution, let alone iterating optimally.

The obvious difficulty with this line of reasoning is that one does not know the correct G, and hence cannot choose the "best" α. One can however always choose α so that, whether a solution exists or not, one iterates toward a solution or towards minimum error. One does this by choosing α to minimize the deviation of G_{out} from G_{in}.

We take as our norm,

$$\int_0^\infty dr\,[G_{\text{in}}(r) - G_{\text{out}}(r)]^2 = \| G_{\text{in}} - G_{\text{out}} \|^2 . \tag{B3}$$

We wish, then, to choose α so as to minimize the difference $\| G_{\text{in}} - G_{\text{out}} \|^2$.

Taking $G_{\text{in}} = \alpha G_0 + (1-\alpha) G_1$ and using Eq. (B1), it follows that

$$G_{\text{out}}(r) = 1 + n \int s\,ds\,(e^{u(s)} - 1)\,[\alpha G_0(s) + (1-\alpha) G_1(s)] \times \int d\theta\,\alpha [G_0(|\vec{r} - \vec{s}|)\, e^{u(|\vec{r}-\vec{s}|)} - 1] + (1-\alpha)\,[G_1(|\vec{r} - \vec{s}|)\, e^{u(|\vec{r}-\vec{s}|)} - 1] . \tag{B4}$$

Using the notation:

$$\{G_i, G_j\} = n \int d\vec{s}\,(e^{u(s)} - 1)\, G_i(s) \times [G_j(|\vec{r} - \vec{s}|)\, e^{u(|\vec{r}-\vec{s}|)} - 1] . \tag{B5}$$

we may rewrite Eq. (B4)

$$G_{\text{out}} = 1 + \alpha^2 \{G_0, G_0\} + (1-\alpha)^2 \{G_1, G_1\} + \alpha(1-\alpha)\{G_0, G_1\} + \alpha(1-\alpha)\{G_1, G_0\} . \tag{B6}$$

Define

$$G_2(r) = 1 + n \int d\vec{s}\,(e^{u(s)} - 1)\, G_1(s) \times [G_1(|\vec{r} - \vec{s}|)\, e^{u(|\vec{r}-\vec{s}|)} - 1] , \tag{B7}$$

then

$$\{G_0, G_0\} = G_1 - 1 ,$$

and

$$\{G_1, G_1\} = G_2 - 1 , \tag{B8}$$

so that Eq. (B6) becomes

$$G_{\text{out}} = 1 + \alpha^2 (G_1 - 1) + (1-\alpha)^2 (G_2 - 1) + \alpha(1-\alpha)\{G_0, G_1\} + \alpha(1-\alpha)\{G_1, G_0\} . \tag{B9}$$

Now define

$$n \int s\,ds\,[G_0(s) - G_1(s)]\,(e^{u(s)} - 1) \int d\varphi \{[G_0(|\vec{r} - \vec{s}|)\, e^{u(|\vec{r}-\vec{s}|)} - 1] - [G_1(|\vec{r} - \vec{s}|)\, e^{u(|\vec{r}-\vec{s}|)} - 1]\}$$

$$\equiv [G_0, G_1] , \tag{B10}$$

$$= \{G_0, G_0\} + \{G_1, G_1\} - \{G_1, G_0\} - \{G_0, G_1\} . \tag{B11}$$

Using Eqs. (B8) and (B10), we may reduce Eq. (B9) to

$$G_{\text{out}} = 1 + \alpha^2 (G_1 - 1) + (1-\alpha)^2 (G_2 - 1) + \alpha(1-\alpha)\,(G_1 - 1) + (G_2 - 1) - [G_0, G_1] . \tag{B12}$$

Thus

$$G_{\text{out}}(r) = (1-\alpha)\, G_2(r) + \alpha G_1(r) - \alpha(1-\alpha)\,[G_0, G_1] . \tag{B13}$$

The norm (B3) is therefore minimized when α satisfies the cubic equation

$$\lambda_3 \alpha^3 + \lambda_2 \alpha^2 + \lambda_1 \alpha + \lambda_0 = 0 , \tag{B14}$$

where

$$\lambda_3 = 4 \int dr\,[G_0, G_1]^2 ,$$

$$\lambda_2 = -4 \int dr\,[G_0, G_1] \{G_2(r) - 2G_1(r) + G_0(r) - [G_0, G_1]\} , \tag{B15}$$

$$\lambda_1 = 2 \int dr\,[G_2(r) - G_1(r)][G_2(r) - 2G_1(r) + G_0(r)] ,$$

and

$$\lambda_0 = 2 \int dr\, [G_2(r) - 2G_1(r) + G_0(r)]^2 .$$

Determining the mix by the solution of Eq. (B14), one is guaranteed for whatever initially guessed G that the optimized iteration gives successively monotonically decreasing errors. The error may not converge to zero, but it does monotonically decrease. A nonzero result can be taken to indicate the nonexistence of a solution.

The quantity $[G_0, G_1]$ is second order in the error in G. In other words, when we are close to the correct solution, $[G_0, G_1]$ becomes negligible. G_{out} then is the mixture of G_2 and G_1 in the same proportion as the original mixture of G_0 and G_1 in G_{in}. That is to lowest order Eq. (B13) is linear.

Neglecting the second-order sum $[G_0, G_1]$, the optimal requirement [Eq. (39)] reduces to a linear equation for α:

$$\alpha = \frac{\int dr\, [G_2(r) - G_1(r)][G_2(r) - 2G_1(r) + G_0(r)]}{\int dr\, [G_2(r) - 2G_1(r) + G_0(r)]^2} . \tag{B16}$$

Within this approximation calculating G_{out} is no more expensive using the optimized mix than it is with any mix. This approximation works well in practice. Calculating with no approximation requires about twice as much computer time as calculating with an arbitrarily chosen mix.

Since we needed a solution up to the highest possible density, we did not neglect the higher-order terms. It was by this method that the solution was obtained up to $\tilde{n} = 0.11$. The minimum was nonzero in this range, but still small: $\| G_{\text{in}} - G_{\text{out}} \| \approx 10^{-3}$. It soon became unacceptably large when we went beyond this density.

---

*Work supported in part by the NSF through Grant No. DMR74-09661, and No. DMR72-03019 administered by the Materials Research Center of Northwestern University.

[1]M. Bretz, J. G. Dash, D. C. Hickernell, E. O. McLean, and O. E. Vilches, Phys. Rev. A 8, 1589 (1973).

[2]D. E. Hagen, A. D. Novaco, and F. J. Milford, in *Proceedings of the Second International Conference on Adsorption-Desorption Phenomena*, edited by F. Ricca (Academic, New York, (1972).

[3]R. L. Siddon and M. Schick, Phys. Rev. A 9, 907 (1974).

[4]A. Novaco and C. E. Campbell, Phys. Rev. B 11, 2525 (1975).

[5]C. E. Campbell and M. Schick, Phys. Rev. A 3, 691 (1971).

[6]M. D. Miller, C.-W. Woo, and C. E. Campbell, Phys. Rev. A 6, 1942 (1972).

[7]C.-W. Woo and R. L. Coldwell, Phys. Rev. Lett. 29, 1062 (1972).

[8]L. Shen, C.-W. Woo, and H. K. Sim, Phys. Rev. D 10, 1925 (1974); and Phys. Rev. B 14, 1323 (1976).

[9]M. D. Miller and C.-W. Woo, Phys. Rev. A 7, 1322 (1973). Erratum: a factor of 4 is missing from every calculated heat-capacity curve.

[10]D. C. Hickernell, E. O. McLean, and O. E. Vilches, Phys. Rev. Lett. 28, 789 (1972); and E. O. McLean, Ph.D. thesis (University of Washington, 1972) (unpublished).

[11]K. S. Liu, M. H. Kalos, and G. V. Chester, Phys. Rev. B 13, 1971 (1976).

[12]D. N. Lowy and C.-W. Woo, Phys. Lett. 56A, 402 (1976); Phys. Rev. B 13, 3790 (1976); Phys. Rev. D 13, 3201 (1976).

[13]See for example C.-W. Woo, in *Physics of Liquid and Solid Helium*, edited by K. H. Bennemann and J. B. Ketterson (Wiley-Interscience, New York, 1976).

[14]M. Born and H. S. Green, Proc. R. Soc. A 188, 10 (1946).

[15]J. K. Percus and G. J. Yevick, Phys. Rev. 110, 1 (1958).

[16]H. Namaizawa (private communication).

[17]R. O. Watts, J. Chem. Phys. 48, 50 (1968).